

## Room temperature photoluminescence of BCT prepared by Complex Polymerization Method

F.V. Motta <sup>a,\*</sup>, A.P.A. Marques <sup>b</sup>, J.W.M. Espinosa <sup>c</sup>, P.S. Pizani <sup>d</sup>, E. Longo <sup>a</sup>, J.A. Varela <sup>a</sup>

<sup>a</sup> LIEC, Departamento de Físico-química, Instituto de Química, Universidade Estadual Paulista, R. Francisco Degni, s/n, Bairro Quitandinha, 14801-907 Araraquara-SP, Brazil

<sup>b</sup> LIEC, Departamento de Química, Universidade Federal de São Carlos, P.O. Box 676, 13565-905 São Carlos, SP, Brazil

<sup>c</sup> Departamento de Engenharia de Produção, Universidade Federal de Goiás, 75704-020 Catalão, GO, Brazil

<sup>d</sup> Laboratório de Semicondutores, Departamento de Física, Universidade Federal de São Carlos, 13565-905 São Carlos, SP, Brazil

### ARTICLE INFO

#### Article history:

Received 7 November 2008

Received in revised form 6 April 2009

Accepted 7 April 2009

Available online 11 April 2009

#### PACS:

77.84.Dy

64.60.Cn

81.40.Tv

78.55.Qr

#### Keywords:

Barium calcium titanate

Order–disorder transition

Optical properties

Photoluminescence

### ABSTRACT

It was used the Complex Polymerization Method to synthesize barium calcium titanate powders (BCT). Crystalline  $\text{Ba}_{0.8}\text{Ca}_{0.2}\text{TiO}_3$  perovskite-type phase could be identified by X-ray diffraction and confirmed by Raman spectroscopy in the powders heat treated at 600 °C. Inherent defects, linked to structural disorder, facilitate the photoluminescence emission. The photoluminescent emission peak maximum was around of 533 nm (2.33 eV) for the  $\text{Ba}_{0.8}\text{Ca}_{0.2}\text{TiO}_3$ . The photoluminescence process and the band emission energy photon showed dependence of both the structural order–disorder and the thermal treatment history. The results revealed that  $\text{Ba}_{0.8}\text{Ca}_{0.2}\text{TiO}_3$  (BCT20) is a highly promising candidate material for optical applications.

© 2009 Elsevier B.V. All rights reserved.

## 1. Introduction

The barium titanate ( $\text{BaTiO}_3$ ) perovskite, that is one ferroelectrics material, has been extensively studied due several possible applications such as electronic and optical devices [1–4]. The substitution of Ba by Ca in the  $\text{BaTiO}_3$  perovskite results in an improvement of the stability of the piezoelectric properties, consequently the barium calcium titanate ( $\text{Ba}_{1-x}\text{Ca}_x\text{TiO}_3$ ) solid solution has attracted great attention for use in the laser systems, electro–optic material for various photorefractive and holographic applications [5–8].

$\text{Ba}_{1-x}\text{Ca}_x\text{TiO}_3$  (BCT) has usually been prepared by the solid state reaction method. In the solid state reaction method the mixture of  $\text{BaCO}_3$ ,  $\text{CaCO}_3$  and  $\text{TiO}_2$  is heat treated at high temperatures for long times and requires two successive calcinations to get high solubility of  $\text{Ca}^{+2}$  in the  $\text{BaTiO}_3$  matrix [9–11]. It has been observed that  $\text{Ca}^{+2}$  replaces  $\text{Ba}^{+2}$  in  $\text{Ba}_{1-x}\text{Ca}_x\text{TiO}_3$  to form tetragonal BCT solid solutions when  $x$  is less than  $\sim 0.23$  [5,12]. Moreover, Cheng and

Shen [12] obtained pure tetragonal phase for  $x \leq 0.25$  and mixture of phases for  $x$  in the range of 0.3–0.85. The synthesis by soft-chemical methods, as the Complex Polymerization Method (CPM), used to synthesize high pure  $\text{BaTiO}_3$  powders, occur at lower temperature than the solid state reaction method. The immobilization of the metal complexes in such rigid organic polymeric networks can reduce the metal segregation, thus ensuring the compositional homogeneity at the molecular scale [13,14].

Jastrabik et al. [8] reported the photoluminescence (PL) and optical absorption in the pure and Cr-doped  $\text{Ba}_{0.77}\text{Ca}_{0.23}\text{TiO}_3$  single crystals at temperatures of the 5–300 K in the 300–800 nm spectral. Interband excitation of pure BCT crystals at  $\lambda = 350$  nm results in the well-known visible wide-band emission with a maximum at  $\sim 552$  nm (green) at 10 K.

Photoluminescence property at room temperature occurs due to structural disorder existing in the perovskite system [15,16]. However, the system can not be fully disordered owing to present a minimal order in the structure. This means that there is an order–disorder rate which favors the PL phenomenon in the system. It has been demonstrated that a series of structurally disorder titanates synthesized by a soft-chemical process have shown intense photo-

\* Corresponding author. Fax: +55 16 33518214.

E-mail address: [fabiana@liec.ufscar.br](mailto:fabiana@liec.ufscar.br) (F.V. Motta).

luminescence (PL) at room temperature [17–19]. In such cases, a minimal order in the system is necessary for the material exhibit PL property at room temperature.

In previous PL studies, the analysis of X-ray absorption near-edge structure (XANES) spectra pointed out the coexistence of two types of environments for titanium atoms, namely, fivefold ( $\text{TiO}_5$ ) square–base pyramid or trigonal bipyramidal and sixfold coordination ( $\text{TiO}_6$ ) octahedron. The order parameter is related to the presence of  $\text{TiO}_6$  clusters, whereas the disorder is related to the presence of  $\text{TiO}_5$  clusters. It is believed that PL occurs due to interaction of  $\text{TiO}_5$ – $\text{TiO}_6$  clusters [20,21]. de Figueiredo et al. [22] observed the PL phenomenon in  $\text{Ca}_{0.95}\text{Sm}_{0.05}\text{TiO}_3$  (CT:Sm) only in disordered structure. Experimental observations suggest that PL emission of CT:Sm is related both to the  $\text{TiO}_5$ – $\text{TiO}_6$  and  $\text{CaO}_{11}$ – $\text{CaO}_{12}$  concentrations; consequently, depends on both the modifier lattice (Ca and Sm ions) and the former lattice (Ti ions) [22,23].

Considering that the CPM is efficient to promote produce structural order–disorder complexes oxides powders and few have has been reported about the property PL of the barium calcium titanate (BCT). This paper reports the synthesis and the structural effect of  $\text{Ba}_{0.8}\text{Ca}_{0.2}\text{TiO}_3$  (BCT20) powders in the conditions that favor the PL emission at room temperature.

## 2. Experimental detail

BCT20 was prepared by CPM [24,25]. In this synthesis, the titanium citrate was prepared by dissolution of titanium (IV) isopropoxide in aqueous solutions of citric acid (CA). This solution was mixed in a stoichiometric molar proportion of 4:1 CA:titanium. The citrate solution was homogenized under constant stirring at a temperature of  $\sim 80$ – $90$  °C, pH  $\sim 1.5$ . After complete dissolution were added  $\text{BaCO}_3$  and  $\text{CaCO}_3$ . Ammonium hydroxide was used to adjust the pH of the solution (pH 7–8). The molar ratio between barium, calcium and titanium cations was 0.80:0.20:1. After homogenization of this solution was added ethylene glycol to promote the polymerization.

After partial evaporation of the water, the polymeric resin was heat treated at 300 °C (10 °C/min) for 4 h, forming an expanded resin, constituted of partially pyrolyzed material. The resin became a dark-brown powder and was crystallized at several temperatures between 400 and 700 °C for 2 h using a heating rate of 5 °C/min.

BCT20 powders were characterized by X-ray diffraction (XRD) using  $\text{Cu K}\alpha$  radiation in order to determine the structural evolution and the lattice parameters  $a$  and  $c$ . The average crystallite diameter ( $D_{\text{cryst}}$ ) was determined by XRD, from the (1 0 1) and (1 1 0) diffraction peaks of the  $\text{BaTiO}_3$  phase ( $2\theta$  at around  $31.5^\circ$  and  $31.6^\circ$ , respectively), according to the Scherrer equation as described by Suryanarayana and Norton [26].

The Raman spectroscopy data were obtained at room temperature by a RFS/100/S Bruker FT-Raman equipment attached to a Nd:YAG laser promoting an excitation light of 1064 nm with spectral resolution of  $4\text{ cm}^{-1}$  and range of 0–1100  $\text{cm}^{-1}$ .

The photoluminescence (PL) spectra of the BCT20 powders were collected with a U1000 Jobin-Yvon double monochromator coupled to cooled GaAs photomultiplier and a conventional photon counting system. The 488.0 nm exciting wavelength of an argon ion laser was used. The maximum output power of the laser was 20 mW. All measurements were taken at room temperature.

## 3. Results and discussion

Fig. 1 shows the XRD patterns of the BCT20 powders heat treated at different temperatures, from 400 to 700 °C. In this figure, it is observed that the BCT20 heat treated at 400 °C is disordered. The materials heat treated between 450 and 550 °C present only broad

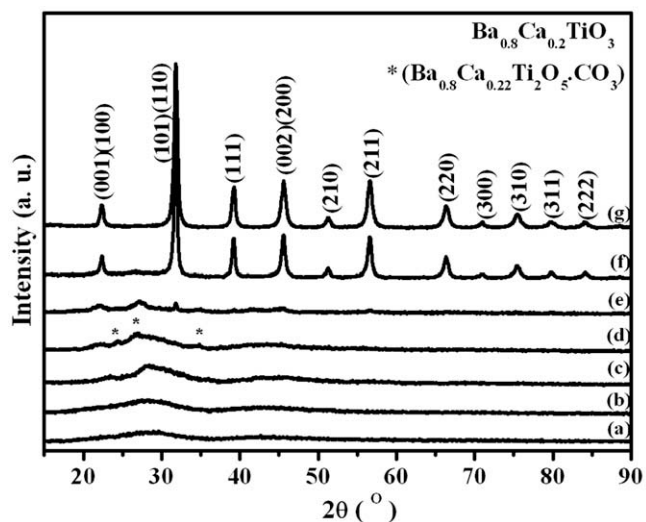


Fig. 1. X-ray diffraction patterns of  $\text{Ba}_{0.8}\text{Ca}_{0.2}\text{TiO}_3$  powders heat treated at (a) 400 °C, (b) 450 °C, (c) 500 °C, (d) 550 °C, (e) 575 °C, (f) 600 °C and (g) 700 °C.

diffraction reflections at  $2\theta \sim 24.3^\circ$ ,  $26.7^\circ$  and  $34.7^\circ$  referent to the barium titanium oxycarbonate,  $(\text{Ba}_{0.8}\text{Ca}_{0.2})_2\text{Ti}_2\text{O}_5 \cdot \text{CO}_3$  [27]. This barium titanium oxycarbonate is an intermediate metastable phase that disappears when the material is heat treated at 575 °C, remaining only the reflections referent to  $\text{Ba}_{0.8}\text{Ca}_{0.2}\text{TiO}_3$  perovskite-type phase. These XRD patterns indicate that the powders samples heat treated at 575 °C and higher temperatures are structurally ordered at long range.

The pure  $\text{BaTiO}_3$  (BT) ceramic shows a tetragonal phase as identified and indexed using the standard XRD data of the corresponding BCT20 powders [5,9]. The lattice parameters and the mean crystallite sizes were calculated from the peak positions displayed in Fig. 1. The ordered BCT20 calculated crystallite sizes were around of 17 nm. The lattice parameters  $a$  and  $c$  were obtained using the least square refinement from the REDE93 program. The lattice parameters  $a$  and  $c$  were around of 3.9607(3) and 3.9941(3) Å, respectively; similar to the values reported for  $\text{Ba}_{0.773}\text{Ca}_{0.227}\text{TiO}_3$  crystals ( $a = 3.962$  Å and  $c = 3.999$  (Å)) [5].

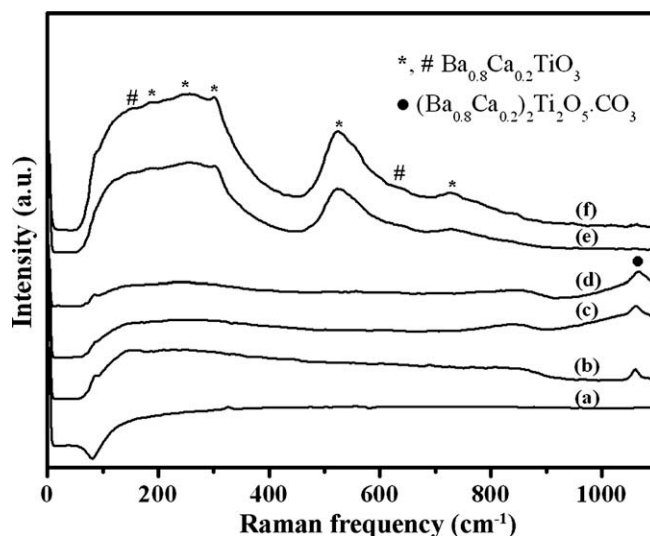


Fig. 2. Spontaneous Raman spectra of BCT20 powders heat treated at (a) 400 °C, (b) 500 °C, (c) 550 °C, (d) 575 °C, (e) 600 °C and (f) 700 °C.

Fig. 2 depicts spontaneous Raman spectra of BCT20 powders recorded at the room temperature for samples calcined from 400–700 °C. The samples heat treated at 400 and 450 °C no present well-resolved sharp peaks in the Raman spectra, indicating that the material is structurally disordered at short range. The Raman spectra of powders heat treated between 500 and 575 °C exhibited a fluorescent-like background. The band around of 1061 cm<sup>-1</sup> (marked with a ● in Fig. 2) was attributed to the (Ba<sub>0.8</sub>Ca<sub>0.2</sub>)<sub>2</sub>Ti<sub>2</sub>O<sub>5</sub> · CO<sub>3</sub> intermediate phase [14]. Bands of the intermediate phase disappear completely in the powders heat treated at 600 and 700 °C, agreeing with XRD data. These alterations were accompanied by appearance of five distinct broad bands referent to the BaTiO<sub>3</sub> *P4 mm* tetragonal phase: 726, 526, 304, 256 and 186 cm<sup>-1</sup> with its respective vibration modes A<sub>1</sub>(LO<sub>3</sub>), A<sub>1</sub>(TO<sub>3</sub>), E (TO), A<sub>1</sub>(TO<sub>2</sub> and A<sub>1</sub>(TO<sub>1</sub>) (marked with a \* in Fig. 2) [2,14]. The Raman peaks at 153 and 640 cm<sup>-1</sup> (marked with a # in Fig. 2) were attributed to the satellite peaks, according to Cho [2], however these peaks can be attributed too the BaTiO<sub>3</sub> hexagonal phase.

The photoluminescence spectra recorded at room temperature for BCT20 powders heat treated at 400–700 °C for 2 h (Fig. 3). BCT20 heat treated at 400–575 °C presented PL emission. The broad and intense band emission covering a large part of the visible spectra, from ~504 to 720 nm was observed for BCT20 powders. The best PL property with the band centered at ~533 nm (2.33 eV) was for the sample heat treated at 500 °C for 2 h. The system has a totally ordered structure (samples annealed at 600 and 700 °C), the PL emission is not observed.

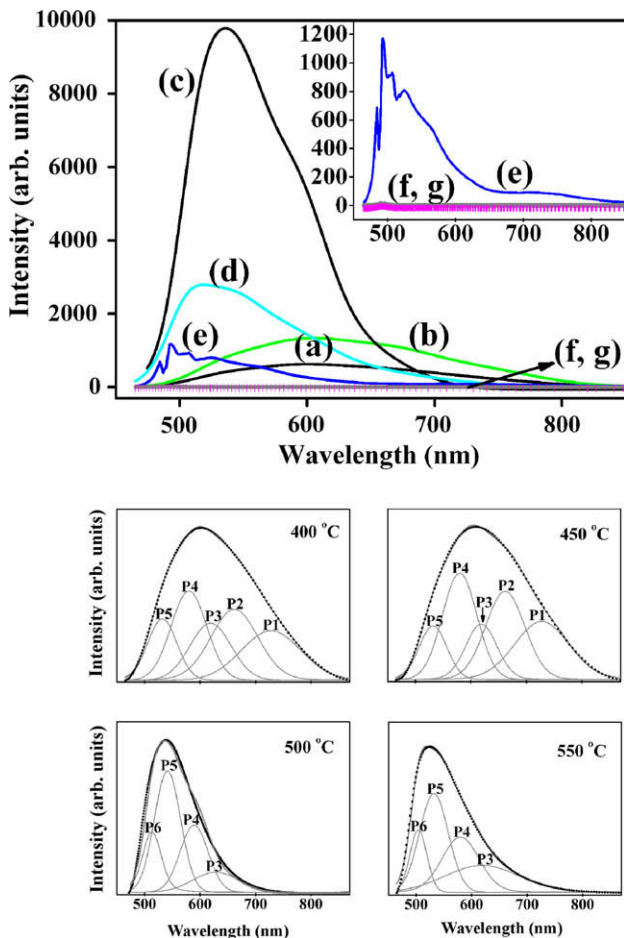


Fig. 3. Room temperature PL spectra of BCT20 powders annealed at (a) 400 °C, (b) 450 °C, (c) 500 °C, (d) 550 °C, (e) 575 °C, (f) 600 °C and (g) 700 °C, obtained with excitation at 488 nm. Deconvolution of PL curve fitted for the samples annealed at 400 °C, 450 °C, 500 °C, and 550 °C.

This profile of the emission band is typical of a multiphonon process, i.e. a system in which relaxation occurs by several paths, involving the participation of numerous states within the band gap of the material [20]. This behavior is related to the structural disorder of BCT20 and indicates the presence of additional electronic levels in the forbidden band gap of the material.

The complex PL band spectra may be due to several components and generally can be **deconvoluted** in individual components. The spectrum is **deconvoluted** based on the nature of the process governing each component. The luminescence process is generally described by a Gaussian line broadening mechanism in which case, the luminescence intensity can be expressed in terms of a Gaussian (amplitude version) line-shape function and can be written by the following equation:

$$I(h\nu) = I_0 + \sum_{i=1}^n A_i \exp \left[ -\frac{(h\nu) - E_{0i}}{2\sigma_i^2} \right], \quad (1)$$

where  $h\nu$  is the energy of the radiation emitted,  $I_0$  is the offset intensity,  $A_i$  is the amplitude of each component,  $E_{0i}$  is the energy of each component in which the intensity is maximum, and  $\sigma_i$  is the standard derivation for each component (FWHM) [28].

In this sense, to have a better understanding of the PL properties and its dependence on the structural order–disorder of the lattice, the PL curves were analyzed using a **deconvolution** program of PickFit [29]. We believe that the PL curves shown in Fig. 3 are composed by six PL components, here named blue–green component (~ 504 nm), green component (~ 532 nm), yellow component (~ 580 nm), orange component (~ 619 nm) and red component (maximum below 662 and 728 nm) in allusion to the region where the maxima of component appears. Each color represents different types of electronic transition and is linked to a specific structural arrangement. The features extracted from **deconvolution** curves and the areas under of respective transitions are listed in Table 1 and illustrated in Fig. 4. The PL **deconvolution** (Fig. 3) shows the BCT20 disordered to ordered structure changing with the annealing increase, favoring the green light emission (smaller wavelength) for higher energies.

In the structure perovskite-type the lattice former titanium is at the center of the cube, surrounded by six oxygens that occupy the middle of the faces, in a regular octahedral configuration. However, the structure before of get its ideal configuration (totally ordered) is a mixture of TiO<sub>5</sub>–TiO<sub>6</sub> clusters intercalated by Ba and Ca atoms. The higher the heat treatment temperature, the more frequent the TiO<sub>6</sub> conformation and the more ordered the structure. The red component decrease with the higher of treatment temperature (ordered structural) and the green component increase. According XRD results the BCT20 powders are ordered annealed at 600 and 700 °C. The ordered powders where only TiO<sub>6</sub> clusters tend to exist does not allow the creation of point defects and do not presents PL emission at room temperature [22]. Similar to the CT:Sm studied by de Figueiredo et al. [22], the compound with intermediary range disorder (500 °C) presented intense PL emission while compared to the compound disordered (400 and 450 °C) and the ordered compound no PL property was showed.

X-ray Absorption Near Edge Structure (XANES) experimental results [30] pointed that the oxygen vacancies in titanates can occur in three different charge states: the [TiO<sub>5</sub> · V<sub>O</sub><sup>x</sup>] complex states, which is neutral relative and presents two electrons paired, the singly ionized [TiO<sub>5</sub> · V<sub>O</sub><sup>-</sup>] complex state, that has one electron despaired, and the doubly positively charged [TiO<sub>5</sub> · V<sub>O</sub><sup>2+</sup>] complex state, which did not trap any electrons.

Before donor excitation, a hole in the acceptor and an electron in a donor are created, according to equations using Kröger–Vink notation [31]:

**Table 1**

The fitting parameters of the Gaussian peaks for PL obtained with excitation wavelength at 488 nm.

T (°C)	Peak center (nm)					
	(P1) 728% <sup>a</sup>	(P2) 662% <sup>a</sup>	(P3) 619% <sup>a</sup>	(P4) 580% <sup>a</sup>	(P5) 532% <sup>a</sup>	(P6) 504% <sup>a</sup>
400	21	27	14	25	12	0
450	21	26	16	25	12	0
500	0	0	17	27	45	11
550	0	0	22	30	36	12

T = temperature of heat annealing; 728 and 662 nm = red component of PL; 619 = orange component of PL; 580 nm = yellow component of PL; 532 = green component of PL and 504 nm = blue–green component of PL.

<sup>a</sup> Obtained dividing the area of each **deconvoluted** PL curves by the total PL area.

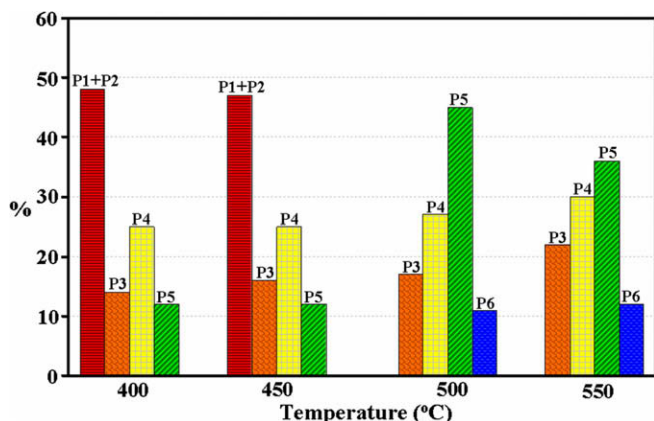
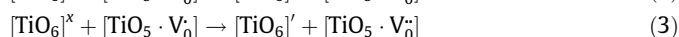


**Fig. 4.** Schematic diagram of the each color contribution after **deconvolution** of PL spectra.



where  $[\text{TiO}_6]$  is donor,  $[\text{TiO}_5 \cdot \text{V}_0]$  is donor–acceptor and  $[\text{TiO}_5 \cdot \text{V}_0^x]$  is acceptor.

These equations suggest that to the transition of a valence-band hole in the conduction band is a necessary requirement the oxygen-vacancy-trapped electron in the valence band. This means that most of electrons around oxygen vacancies are released and, therefore, such oxygen vacancy complex site is relatively positive charged. Moreover, oxygen vacancies tend to trap photo-generated electrons. The charge transfer occurring as proposed in Eqs. (2)–(4) create electrons and hole polarons that can be designed as bipolarons. After the photon excitation, the recombination and decay process follow the many valid hypotheses presented in the literature [32]. The present work shows that the emission process leading to PL is facilitated by previous existence of these complex clusters in the ground state. The order–disorder BCT20 powders thus intrinsically possess the necessary condition for creating PL at room temperature.

#### 4. Conclusions

Powders of BCT20 have been synthesized following by CPM. The ordering system at short and long range was accompanied for the  $\text{Ba}_{0.8}\text{Ca}_{0.2}\text{TiO}_3$  using Raman, PL band and XRD characterization. Raman data related to short-range and XRD results at long-range order shows that the material is organized at 600 °C. However, the phenomenon of PL at room temperature is not observed in the order structure at 600 °C. The introduction of  $\text{Ca}^{+2}$  ion in  $\text{BaTiO}_3$  proportioned intrinsic defects. These intrinsic defects, linked to

structural disorder, facilitate the main emission process to PL. Disorder in solids provokes degeneracy and destabilization in the localized states of the atoms acting as electron-hole pairs and supporting the broad PL band phenomena and electronic levels are fundamental to understanding the order–disorder process in the solid state. These optical properties exhibited by disordered BCT20 suggest that this material is a highly promising candidate for photoluminescent applications.

#### Acknowledgements

The authors gratefully acknowledge the financial support of the Brazilian research financing institutions: CAPES, CNPq and FAPESP-CEPID.

#### References

- [1] Z.G. Shen, J.F. Chen, J. Yun, *J. Cryst. Growth* 267 (2004) 325.
- [2] W.S. Cho, *J. Phys. Chem. Solids* 59 (1998) 659.
- [3] P. Kantha, K. Pengpat, P. Jarupoom, U. Intatha, G. Rujijanagul, T. Tunkasiri, *Curr. Appl. Phys.* 9 (2009) 460.
- [4] S. Kongtaweelert, D.C. Sinclair, S. Panichphant, *Curr. Appl. Phys.* 6 (2006) 474.
- [5] C. Kuper, R. Pankrath, H. Hesse, *Appl. Phys. A-Mater. Sci. Process.* 65 (1997) 301.
- [6] S. Bernhardt, H. Veenhuis, P. Delaye, R. Pankrath, G. Roosen, *Appl. Phys. B-Lasers Opt.* 72 (2001) 667.
- [7] N. Korneev, D. Mayorga, S. Stepanov, H. Veenhuis, K. Buse, C. Kuper, H. Hesse, E. Kratzig, *Opt. Commun.* 160 (1999) 98.
- [8] L. Jastrabik, S.E. Kapphan, V.A. Trepakov, I.B. Kudyk, R. Pankrath, *J. Lumin.* 102 (2003) 657.
- [9] X.M. Chen, I. Wang, J. Li, *Mater. Sci. Eng. B* 113 (2004) 117.
- [10] M.C. Chang, S.C. Yu, *J. Mater. Sci. Lett.* 19 (2000) 1323.
- [11] T. Suzuki, M. Ueno, Y. Nishi, M. Fujimoto, *J. Am. Ceram. Soc.* 84 (2001) 200.
- [12] X. Cheng, M. Shen, *Mater. Res. Bull.* 42 (2007) 1662.
- [13] M. Kakhana, M. Arima, Y. Nakamura, M. Yashima, M. Yoshimura, *Chem. Mater.* 11 (1999) 438.
- [14] P. Duran, D. Gutierrez, J. Tartaj, M.A. Banares, C. Moure, *J. Eur. Ceram. Soc.* 22 (2002) 797.
- [15] F.M. Pontes, E. Longo, E.R. Leite, E.J.H. Lee, J.A. Varela, P.S. Pizani, C.E.M. Campos, F. Lanciotti, V. Mastelaro, C.D. Pinheiro, *Mater. Chem. Phys.* 77 (2003) 598.
- [16] E. Orhan, J.A. Varela, A. Zenatti, M.F.C. Gurgel, F.M. Pontes, E.R. Leite, E. Longo, P.S. Pizani, A. Beltran, J. Andres, *Phys. Rev. B* 71 (2005) 085113.
- [17] P.S. Pizani, H.C. Basso, F. Lanciotti, T.M. Boschi, F.M. Pontes, E. Longo, E.R. Leite, *Appl. Phys. Lett.* 81 (2002) 253.
- [18] E. Orhan, V.C. Albarici, M.T. Escote, M.A.C. Machado, P.S. Pizani, E.R. Leite, J.R. Sambrano, J.A. Varela, E. Longo, *Chem. Phys. Lett.* 398 (2004) 330.
- [19] V.M. Longo, L.S. Cavalcante, A.T. de Figueiredo, L.P.S. Santos, E. Longo, J.A. Varela, J.R. Sambrano, C.A. Paskocimas, F.S. De Vicente, A.C. Hernandez, *Appl. Phys. Lett.* 90 (2007) 091906.
- [20] P.S. Pizani, E.R. Leite, F.M. Pontes, E.C. Paris, J.H. Rangel, E.J.H. Lee, E. Longo, P. Delega, J.A. Varela, *Appl. Phys. Lett.* 77 (2000) 824.
- [21] V. Mastelaro, P.P. Neves, S.R. de Lazaro, E. Longo, A. Michalowicz, J.A. Eiras, *J. Appl. Phys.* 99 (2006) 1.
- [22] A.T. de Figueiredo, V.M. Longo, S. de Lazaro, V.R. Mastelaro, F.S. De Vicente, A.C. Hernandez, M. Siu Li, J.A. Varela, E. Longo, *J. Lumin.* 126 (2007) 403.
- [23] A.T. de Figueiredo, S. de Lazaro, E. Longo, E.C. Paris, J.A. Varela, M.R. Joya, P.S. Pizani, *Chem. Mater.* 18 (2006) 2904.
- [24] V.S. Marques, L.S. Cavalcante, J.C. Sczacoski, D.P. Volanti, J.W.M. Espinosa, M.R. Joya, M.R.M.C. Santos, P.S. Pizani, J.A. Varela, E. Longo, *Solid State Sci.* 10 (2008) 1056.
- [25] F.V. Motta, A.P.A. Marques, M.T. Escote, D.M.A. Melo, A.G. Ferreira, E. Longo, E.R. Leite, J.A. Varela, *J. Alloys Compd.* 465 (2008) 452.

- [26] C. Suryanarayana, M.G. Norton, *X-ray Diffraction: A Practical Approach*, Plenum Press, New York, 1998.
- [27] S. Kumar, G.L. Messing, W.B. White, *J. Am. Ceram. Soc.* 76 (1993) 617.
- [28] R.A. Street, *Adv. Phys.* 25 (1976) 397;  
P.R. Bevington, *Data Reduction and Error Analysis for the Physical Sciences*, Mc-Graw-Hill, New York, 1969.
- [29] T. Ding, W.T. Zheng, H.W. Tian, J.F. Zang, Z.D. Zhao, S.S. Yu, X.T. Li, F.L. Meng, Y.M. Wang, X.G. Kong, *Solid State Commun.* 132 (2004) 815.
- [30] K. Asokan, J.C. Jan, J.W. Chiou, W.F. Pong, P.K. Tseng, I.N. Lin, *J. Synchrot. Radiat.* 8 (2001) 839.
- [31] F.A. Kröger, H.J. Vink, in: F. Seitz, D. Turnbull (Eds.), *Solid State Physics*, third ed., Academic Press, New York, 1956, p. 307.
- [32] R. Leonelli, J.L. Brebner, *Solid State Commun.* 54 (1985) 505.